Experimental investigation of continuous-variable quantum teleportation
— Source link ↗

Warwick P. Bowen, Nicolas Treps, Ben C. Buchler, Roman Schnabel ...+4 more authors

Institutions: Australian National University, University of Queensland

Topics: Quantum teleportation, Teleportation, Quantum entanglement and Quantum information science

Related papers:

- Unconditional quantum teleportation

- Teleporting an unknown quantum state via dual classical and Einstein-Podolsky-Rosen channels

- Quantum teleportation of light beams

- Teleportation of Continuous Quantum Variables

- Experimental quantum teleportation

Experimental investigation of continuous-variable quantum teleportation

Warwick P. Bowen,[1] Nicolas Treps,[1] Ben C. Buchler,[1] Roman Schnabel,[1] Timothy C. Ralph,[2] Hans-A. Bachor,[1] Thomas Symul,[1] and Ping Koy Lam[1]

[1]*Department of Physics, Faculty of Science, Australian National University, Canberra ACT 0200, Australia*
[2]*Department of Physics, Centre for Quantum Computer Technology, University of Queensland, St Lucia, Queensland 4072, Australia*

We report the experimental demonstration of quantum teleportation of the quadrature amplitudes of a light field. Our experiment was stably locked for long periods, and was analyzed in terms of fidelity $\mathcal{F}$ and with signal transfer $T_q = T^+ + T^-$ and noise correlation $V_q = V^+_{\text{in}|\text{out}} V^-_{\text{in}|\text{out}}$. We observed an optimum fidelity of 0.64 ± 0.02, $T_q = 1.06 \pm 0.02$, and $V_q = 0.96 \pm 0.10$. We discuss the significance of both $T_q > 1$ and $V_q < 1$ and their relation to the teleportation no-cloning limit.

Quantum teleportation [1] is a key part of quantum information technology both in terms of communicating [2] and processing [3] quantum information. Experimental demonstrations of teleportation have so far fallen into three main categories: teleportation of photon states [4]; of ensemble properties in liquid NMR [5]; and of optical-field states [6]. An important feature of the technique used in the optical-field state experiment of Furusawa *et al.* [6] is its high efficiency. This results in the ability to faithfully teleport arbitrary input states continuously. This is due to the in principle ability to perform the required joint measurements exactly and the technical maturity of optical-field detection. In contrast, the efficiency of single-photon experiments is presently restricted in principle due to the inability to identify all four Bell states, and also in practice by the low efficiency of single-photon production and detection.

Since the Furusawa *et al.* experiment, there have been many proposals for how quantum teleportation may be repeated using different systems [7–9]; applied to different input states [10,11]; generalized to multiparty situations [12]; and more comprehensively characterized [13,14]. Inspite of the considerable interest, to date no new experiment has been performed [15].

This paper reports the quantum teleportation of the quadrature amplitudes of a light beam. Our scheme has a number of notable differences to the previously published experiment. The input and output states are analyzed by the same homodyne detector, allowing a more consistent evaluation of their properties. Our experiment is based on a Nd:YAG (yttrium aluminum garnet) laser that produces two squeezed beams in two independently pumped optical-parametric amplifiers (OPAs). We use a more compact configuration for Alice's measurements. Finally, the encoding and decoding of the input and output signals uses a total of four independent modulators. This allows us to completely span the phase space of the input state.

We analyze our results using the fidelity $\mathcal{F}$ between the input and output states, and also with signal transfer T_q and noise correlation V_q in a manner analogous to quantum nondemolition analysis [7] (which we refer to as the *T-V* measure henceforth). This enables us to give a more detailed characterization of the performance of our teleporter.

Teleportation is usually described as the disembodied transportation of an *unknown quantum state* from one place (Alice) to another (Bob). In our experiment, as in Ref. [6], the teleported states are modulation sidebands of a bright optical beam. The teleportation process can be described using the field annihilation operator $\hat{a} = (\hat{X}^+ + i\hat{X}^-)/2$ where $\hat{X}^\pm = 2\alpha^\pm + \delta\hat{X}^\pm$ are the amplitude $(+)$ and phase $(-)$ quadratures of the field, $\alpha^\pm = \langle \hat{X}^\pm \rangle / 2$ are the real and imaginary parts of the coherent amplitudes, and $\delta\hat{X}^\pm$ are the quadrature noise operators. Throughout this paper, the variances of these noise operators are $V^\pm = \langle \delta\hat{X}^{\pm 2} \rangle$. The fidelity can be evaluated from the overlap of the input (in) and output (out) states, and for the Gaussian states is given by

$$\mathcal{F} = 2e^{-(k^+ + k^-)} \sqrt{\frac{V^+_{\text{in}} V^-_{\text{in}}}{(V^+_{\text{in}} + V^+_{\text{out}})(V^-_{\text{in}} + V^-_{\text{out}})}}, \quad (1)$$

where $k^\pm = \alpha^{\pm 2}_{\text{in}}(1 - g^\pm)^2/(V^\pm_{\text{in}} + V^\pm_{\text{out}})$ and $g^\pm = \alpha^\pm_{\text{out}}/\alpha^\pm_{\text{in}}$ are the teleportation gains. For a sufficiently broad set of coherent states, the best average fidelity at unity gain without entanglement is $\mathcal{F}_{\text{class}} = 0.5$. Another interesting limit is at $\mathcal{F} = 2/3$. This limit guarantees that Bob has the best copy of the input state and is commonly referred to as the *no-cloning limit* [14]. Ideal teleportation would result in $\mathcal{F} = 1$.

Alternatively, quantum teleportation can be defined as the transfer of *quantum information* between Alice and Bob using the *T-V* measure. This more general definition includes cases for which only the useful quantum features of a system have been transferred. In such cases a demonstrably quantum result may be obtained even though other features of the state, for example, the state amplitude, have been distorted sufficiently to degrade fidelity. In the absence of entanglement, strict limits are placed on both the accuracy of measurement and reconstruction of an unknown state. These are the so-called two quantum duties. In contrast to fidelity, the *T-V* measure is state independent and therefore invariant under local symplectic operations.

Bob's reconstruction is limited by the generalized uncertainty principle of Alice's measurement $V^+_M V^-_M \geq 1$ [16], where $V^\pm_M$ are the measurement penalties, which holds for simultaneous measurements of conjugate quadrature ampli-

tudes. In the absence of entanglement, this places a strict limit on Bob's reconstruction accuracy. The limit can be expressed in terms of quadrature signal transfer coefficients [7], $T^{\pm} = \mathcal{R}_{\text{out}}^{\pm}/\mathcal{R}_{\text{in}}^{\pm}$ as

$$T_q = T^+ + T^- - T^+ T^- \left(1 - \frac{1}{V_{\text{in}}^+ V_{\text{in}}^-} \right) \leq 1 \qquad (2)$$

where $\mathcal{R}^{\pm} = \alpha^{\pm}/V^{\pm}$ are the signal-to-noise ratios. For minimum uncertainty input states ($V_{\text{in}}^+ V_{\text{in}}^- = 1$), this expression reduces to $T_q = T^+ + T^-$.

Bob's reconstruction must be carried out on an optical field, the fluctuations of which obey the uncertainty principle. In the absence of entanglement, these intrinsic fluctuations remain present on any reconstructed field. Thus the amplitude and phase conditional variances, $V_{\text{in|out}}^{\pm} = V_{\text{out}}^{\pm} - |\langle \delta \hat{X}_{\text{in}}^{\pm} \delta \hat{X}_{\text{out}}^{\pm} \rangle|^2/V_{\text{in}}^{\pm}$, which measure the noise added during the teleportation process, must satisfy $V_{\text{in|out}}^+ V_{\text{in|out}}^- \geq 1$. This can be written in terms of the quadrature variances of the input and output states and the teleportation gain as

$$V_q = (V_{\text{out}}^+ - g^{+2} V_{\text{in}}^+)(V_{\text{out}}^- - g^{-2} V_{\text{in}}^-) \geq 1. \qquad (3)$$

It should be noted that $(V_{\text{in|out}}^+ + V_{\text{in|out}}^-) \geq 2$ has also been proposed for the conditional variance limit. For cases where both quadratures are symmetric, as considered previously [7,10], both limits are equivalent. The product limit, however, is significantly more immune to asymmetry in the teleportation gain and is, therefore, preferred. The criteria of Eqs. (2) and (3) enable teleportation results to be represented on a T-V graph similar to those used to characterize quantum nondemolition experiments [17].

Both the T_q and V_q limits have independent physical significance. If Bob passes the T_q limit, this forbids any others parties from doing so, therefore, ensuring that the transfer of information to Bob is greater than to any other party. This is an "information cloning" limit that is particularly relevant in light of recent proposals for quantum cryptography [18]. Furthermore, if Bob passes the T_q limit at unity gain ($g^{\pm} = 1$), then Bob has beaten the no-cloning limit and has $\mathcal{F} \geq 2/3$. Surpassing the V_q limit is a necessary prerequisite for reconstruction of nonclassical features of the input state such as squeezing. The T-V measure coincides with the teleportation no-cloning limit at unity gain when both $T_q = V_q = 1$. Clearly it is desirable that the T_q and V_q limits are simultaneously exceeded. Perfect reconstruction of the input state would result in $T_q = 2$ and $V_q = 0$.

The laser source for our experiment was a 1.5 W monolithic nonplanar ring Nd:YAG laser at 1064 nm. Its output was split into two roughly equal power beams. One beam was mode matched into a MgO:LiNbO$_3$ frequency doubler producing 370 mW of 532 nm light. The other beam was passed through a high finesse ring cavity to reduce spectral noise. This spectrally cleaned beam, which was quantum noise limited above 6 MHz, was then used to generate the signal for teleportation; to seed a pair of MgO:LiNbO$_3$ OPAs; and to provide local oscillator beams.
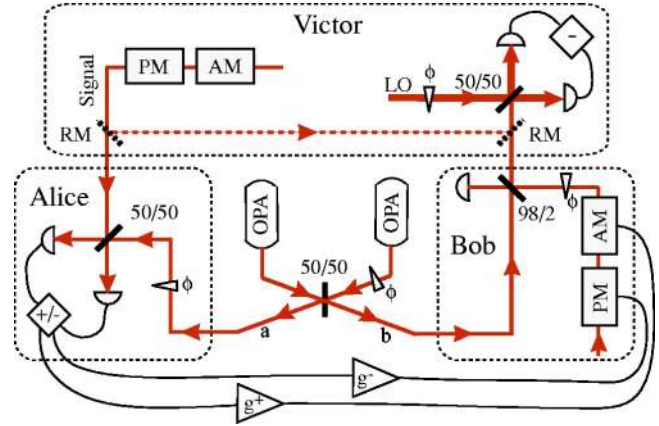

FIG. 1. A schematic diagram of the teleportation experiment. RM, removable mirror; 50/50, symmetric beam splitter; 98/2, 98% transmitting beam splitter; ϕ, phase control; A(P)M, amplitude (phase) modulators.

Our experimental setup to generate entanglement and perform teleportation is shown in Fig. 1. We produced the entanglement by combining a pair of amplitude squeezed beams with a $\pi/2$ phase shift on a 50/50 beam splitter [19]. The squeezed beams were produced by the two OPAs, each pumped with half of the 532 nm light [20]. We characterized the entanglement with the inseparability measure proposed by Duan *et al.* [21]; and obtained the result $[\langle (\hat{X}_a^+ - \hat{X}_b^+)^2 \rangle + \langle (\hat{X}_a^- + X_b^-)^2 \rangle]/2 = 0.44 \pm 0.02$, where subscripts a and b label the two entangled beams; this result is well below the inseparability limit of unity. In our situation, this value becomes equivalent to the average of the squeezed variances of the two OPAs. This corresponds to 3.6 dB of squeezing on each beams. Taking account of 16% loss in post-entanglement optics, we infer 4.8 dB of squeezing at the output of each OPA.

The teleportation experiment (Fig. 1) consisted of three parts: measurement (Alice), reconstruction (Bob), and generation and verification (Victor). At the generation stage, a beam was independently phase and amplitude modulated at 8.4 MHz. Alice then took one of the entangled beams and combined it on a 50/50 beam splitter with the input state with $\pi/2$ phase shift. The intensities of these two beams were balanced so that the sum (difference) of the photocurrents obtained through detection of the two beam splitter outputs provided a measure of the amplitude (phase) quadrature of the input state combined with the entangled beam. These photocurrents were sent electronically to Bob. Bob used them to modulate an independent laser beam that was then combined with the second entangled beam on a 98/2 beam splitter. One output of this beam splitter was Bob's reconstructed output state.

By using removable mirrors, Victor could measure the Wigner functions of both the input and output states. Assuming the states are Gaussian, Victor need only measure the two quadratures to fully characterize the input state. We achieved these measurements in a locked homodyne detector. It is interesting to note that imperfections such as inefficiency and low local oscillator power actually improve the results ob-
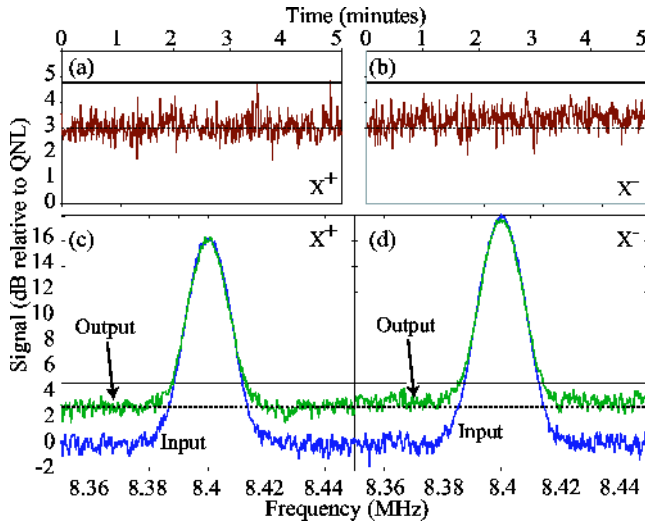
FIG. 2. The input and output states of the teleporter, as measured by Victor. (a) and (b) show the amplitude and phase noise of the output state at 8.4 MHz. (c) and (d) show the input and output of the teleporter, when probed with a signal at 8.4 MHz. In all cases, the dotted line is the no-cloning limit, while the solid line is the classical limit. All data have been corrected to account for the detection losses of Victor. Resolution bandwidth=10 kHz, video bandwidth=30 Hz.

FIG. 3. Measured fidelity plotted; versus teleportation gain, g, in (a) and (b); versus coherent amplitude separation between input and output states in (c); and on phase space in (d). In (a) the input signal size was $(\alpha^+, \alpha^-) \approx (2.9, 3.5)$ and in (b) $(\alpha^+, \alpha^-) \approx (4.5, 5.4)$. g was calculated as the ratio of the input and output coherent amplitudes. The dashed (solid) lines show the classical (no-cloning) limits of teleportation at unity gain. The solid curves are calculated results based on available entanglement, the dot-dashed curves include the experimental asymmetric gains: for (a) $g^- = 0.84g^+$ and for (b) $g^- = 0.92g^+$. In (c) and (d) axes are normalized to the QNL.

tained by Victor. In our analysis, we corrected for these effects.

Active control of the entire experiment required ten locking loops and four temperature control loops. They ensured that the mode cleaner, frequency doubler, two OPA cavities, phases of the OPA pump beams, Alice and Bob phases, Victor homodyne detection, and the relative phase between the squeezed beams were all stably locked. A sample of the data obtained from our teleporter is shown in Fig. 2. Figures 2(a) and 2(b) show the noise of the output state as a function of time. The complete system maintained lock for long periods. The data in Figs. 2(c) and 2(d) show the measurement of the two quadratures over a 100 kHz bandwidth. Over this range the noise floor of the system was constant. The signal-to-noise-ratio was, therefore, found by comparing the peak height at 8.4 MHz to the noise at 8.35 and 8.45 MHz. Every set of teleportation data consisted of four spectra, such as those shown in Fig. 2(c) and 2(d), as well as a quantum noise calibration (not shown). Also drawn in each part of Fig. 2 are lines corresponding to the classical limit (solid line at 4.8 dB) and the no-cloning limit (dashed line at 3 dB). For this dataset, the noise floor of both quadratures lies convincingly below the classical limit and approaches very close to the no-cloning limit. Note that these limits are those calculated for an ideal lossless teleporter. The fidelity obtained for this data was $\mathcal{F}=0.64\pm0.02$.

Figure 3(d) shows the area of phase space that our experiment has probed. All points shown here satisfied $\mathcal{F}>0.5$. For the most part, our input states had nonzero coherent amplitude components, thereby allowing verification of the gains of both quadratures. One of the features of fidelity is a strong dependence on gain and signal size. For example, in the limit of a vacuum input state, the fidelity criterion will actually be
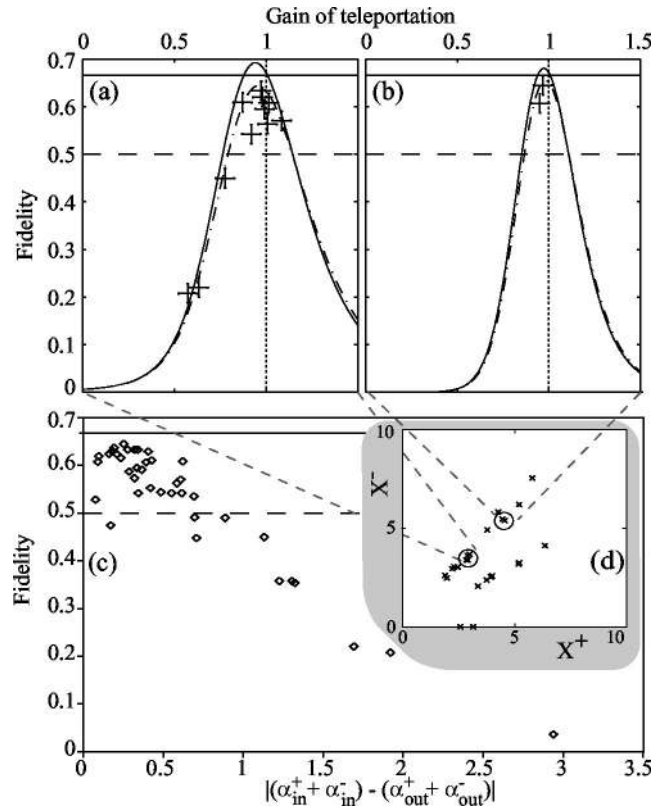
satisfied perfectly by a classical teleporter (i.e., one with the entangled state replaced by two coherent states) with zero gain. The fidelity criterion, therefore, requires proof that the gain of a teleportation event is unity. A subset of our data is shown in Figs. 3(a) and 3(b). Each diagram plots fidelity as a function of teleportation gain for results with identical input states. The solid curves show the best possible performance of our system, based on our entanglement, detection efficiency, dark noise, and assuming equal gain on each quadrature. Both plots demonstrate that the highest fidelity occurs for gain less than unity. The increased fidelity is less obvious in Fig. 3(b) where the signal is approximately twice as large as that in Fig. 3(a). For small signals it is, therefore, crucial to ensure unity gain. Obtaining the correct gain setting is actually one of the more troublesome experimental details. To illustrate this point, we have plotted the dashed curves on Figs. 3(a) and 3(b) for a teleporter with asymmetric quadrature gains. Such asymmetry was not unusual in our system, and explains the variability of the results shown in Fig. 3(a). A summary of all our fidelity results is shown in Fig. 3(c) as a function of deviation from unity gain.

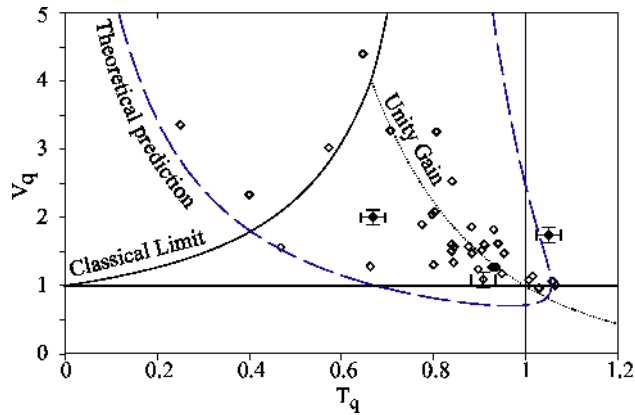Analyzing teleportation results on a T-V graph has several

FIG. 4. T-V graph of the experimental results. The dashed theoretical curve was calculated based on the available entanglement and experimental losses. Representative error bars are shown for some points.

advantages when compared to fidelity. The T-V graph is two dimensional, and, therefore, conveys more information about the teleportation process. It tracks the quantum correlation and signal transfer in nonunity gain situations. In particular, it identifies two particularly interesting regimes that are not evident when using fidelity: the situations where the output state has minimum noise (minimum V_q), and when the input signals were transferred to the output state optimally (maximum T_q). Our T-V results are shown in Fig. 4. The classical limit curve shows the ideal achievable result as a function of gain if the entanglement was replaced with two coherent states. The unity gain curve shows the locus of points obtained at unity teleportation gain with increasing entanglement. Finally, a theoretical curve (as a function of gain) is shown for our experimental parameters. By varying our ex-

perimental conditions, particularly the gain, we have mapped out some portion of the T-V graph.

Perhaps the most striking feature of these results are the points with $T_q > 1$, the best of which has $T_q = 1.06 \pm 0.03$. Since only one party may have $T_q > 1$, this shows that Bob has maximal information about the input signal and we have broken the information cloning limit. The lowest observed conditional variance product was $V_q = 0.96 \pm 0.10$. This point also had $T_q = 1.04 \pm 0.03$. This is the first observation of both $T_q > 1$ and $V_q < 1$, and with unity gain this would imply breaking of the no-cloning limit for teleportation. This particular point, however, had a fidelity of 0.63 ± 0.03. The main reason for this low fidelity is asymmetric gain, the amplitude gain was $g^+ = 0.92 \pm 0.08$, while the phase gain was $g^- = 1.12 \pm 0.08$. Such gain errors have a dramatic impact on the measured fidelity because the output state then has a different classical amplitude ($\alpha^\pm$) to the input, a difference in the classical properties of the input and output states to which fidelity is very sensitive.

In conclusion, we have performed stably locked quantum teleportation of an optical field. The best fidelity, we directly observed was $\mathcal{F} = 0.64 \pm 0.02$. The maximum two quadrature signal transfer for our apparatus was $T_q = 1.06 \pm 0.03$. We also observed a conditional variance product of $V_q = 0.96 \pm 0.10$ coincident with $T_q = 1.04 \pm 0.03$. This is the first observation of both $T_q > 1$ and $V_q < 1$. At unity gain this would ensure violation of the no-cloning limit for teleportation. The asymmetry in our gain, however, prevented a direct measurement of $\mathcal{F} > 0.67$, thereby leaving the no-cloning limit as a tantalising prospect for future experiments.

[1] C.H. Bennett *et al.*, Phys. Rev. Lett. **70**, 1895 (1993).

[2] M. Nielsen and I. Chuang, *Quantum Computation and Quantum Information* (Cambridge University Press, Cambridge, 2000).

[3] D. Gottesman and I.L. Chuang, Nature (London) **402**, 390 (1999).

[4] See, for example, D. Bouwmeester *et al.*, Nature (London) **390**, 575 (1997); D. Boschi *et al.*, Phys. Rev. Lett. **80**, 1121 (1998).

[5] M.A. Nielsen *et al.*, Nature (London) **396**, 52 (1998).

[6] A. Furusawa *et al.*, Science **282**, 706 (1998).

[7] T.C. Ralph and P.K. Lam, Phys. Rev. Lett. **81**, 5668 (1998).

[8] G. Leuchs *et al.*, J. Mod. Opt. **46**, 1927 (1999).

[9] J. Zhang and K. Peng, Phys. Rev. A **62**, 064302 (2000).

[10] R.E.S. Polkinghorne and T.C. Ralph, Phys. Rev. Lett. **83**, 2095 (1999).

[11] T. Ide *et al.*, Phys. Rev. A **65**, 012313 (2002).

[12] P. van Loock and S.L. Braunstein, Phys. Rev. Lett. **84**, 3482 (2000).

[13] T.C. Ralph *et al.*, J. Opt. B: Quantum Semiclassical Opt. **1**, 483 (1999).

[14] F. Grosshans and P. Grangier, Phys. Rev. A **64**, 010301(R) (2001).

[15] With the exception of a recent paper by Zhang *et al.*, on the same optical system used by Furusawa *et al.*, e-print quant-ph/0207076.

[16] E. Arthurs and M.S. Goodman, Phys. Rev. Lett. **60**, 2447 (1988).

[17] P. Grangier *et al.*, Nature (London) **396**, 537 (1998).

[18] F. Grosshans and P. Grangier, Phys. Rev. Lett. **88**, 057902 (2002).

[19] Z.Y. Ou *et al.*, Phys. Rev. Lett. **68**, 3663 (1992).

[20] W. Bowen *et al.*, Phys. Rev. Lett. **88**, 093601 (2002).

[21] L.-M. Duan *et al.*, Phys. Rev. Lett. **84**, 2722 (2000).